# A SEARCH FOR THE $|\Delta S| = 2$ WEAK NON-LEPTONIC DECAY $\Xi^0 \to p\pi^-$

R. Handler and M. Sheaff*

The University of Wisconsin

A. Beretvas and T. Devlin

Rutgers - The State University of New Jersey

K. Heller and T. Joyce

The University of Minnesota

J. Dworkin, O.E. Overseth, G. Valenti

The University of Michigan

* Scientific Spokesman
(608) 262-0804

## Abstract

A search for the $|\Delta S| = 2$ weak non-leptonic decay $\Xi^\circ \to p\pi^-$ is proposed where one event detected corresponds to a branching ratio of $10^{-8}$. This is several orders of magnitude below the present experimental upper limits (90% confidence level) of:

$$\Xi^\circ \to p\pi^- \leq 3.6 \times 10^{-5} \quad \text{(Ref. 1)}$$

$$\Xi^- \to n\pi^- \leq 1.9 \times 10^{-5} \quad \text{(Ref. 2)}.$$

This improvement is made possible by a selective second level trigger processor taking $\leq 1$ $\mu$ sec. per decision. The level to which the test can be made is limited by the instantaneous rates the upstream multi-wire proportional chambers can handle due to space charge effects. A beam time of 500 hours is requested in the Proton Center beam line.

## Introduction

Few predictions for the $|\Delta S| = 2$ decays of hyperons appear in the literature. Those that have been published have resulted from theoretical attempts to describe the CP violations that occur in neutral K decays.[3,4,5] The ordinary V-A current of weak interactions is CP conserving. The small size of the $K_L$-$K_S$ mass difference, $\Delta m \sim 10^{-14} m_k$, restricts any $\Delta S = 2$ vector current, which has C and P even, to be at most second order weak. A $\Delta S = 2$ axial vector current, which has C and P odd, does not contribute to the K mass difference as first pointed out by Glashow[6] and therefore is not restricted by it. Thus the existence of an effective weak Hamiltonian with $\Delta S = 2$ and $P = -1$, whether CP conserving or CP violating, is an open question, accessible only through studies of $\Xi$ and $\Omega^-$ decays.

The CP violating theories with $\Delta S = 2$ fall into two categories: $C = -1$, $P = +1$;[3,4] and $C = +1$, $P = -1$.[5] No CP violating matrix element can contribute appreciably to the $K_L$-$K_S$ mass difference. The first category contains the super-weak theory of Wolfenstein, which produces a branching ratio for $\Xi^\circ \to p\pi^-$ less than that expected from a conventional second order weak interaction ($\sim 10^{-13}$), and is hence negligible. Branching ratios larger than the second order weak interaction could be produced by Okun''s theory, which falls in the second category. It should be emphasized, however, that the observation of $(\Xi^\circ \to p\pi^-)/\text{all}$ in the $10^{-6}$ to $10^{-8}$ range would not of itself be evidence for CP violation, but only for $\Delta S = 2$, $P = -1$. Could such an interaction be accommodated by a current X current theory with weak intermediate bosons?

The usual theoretical framework within the currently favored 6-quark model is the K-M matrix scheme[7] which describes all couplings of the $W^\pm$ and $Z^\circ$ to the quarks. The CP violations occur because there is one free phase available in the theory. The GIM[8] mechanism results in a cancellation of the strangeness changing neutral currents in first order. It

is possible, however, to construct a $\Delta S = 2$ Hamiltonian of current X current form which would occur in first order by postulating couplings to two additional intermediate neutral bosons.[9] They must interfere to kill the CP even, C and P even vector part of Hw which is restricted by the $K_L$-$K_S$ mass difference. Also, they must not couple to leptons or the measured rate for $K_L \rightarrow \mu^+\mu^-$ would be too small. The interaction could be made CP violating by the judicious insertion of an i.

The sections that follow describe an experiment that has been optimized for acceptance of true $\Xi^\circ \rightarrow p\pi^-$ decays, should they occur, at a beam energy of 1000 GeV in the Proton Center neutral hyperon beam. Two crucial questions must be answered in proposing a test several orders of magnitude more sensitive than the existing data allows. One is whether a trigger can be devised which is efficient for true $\Xi^\circ \rightarrow p\pi^-$ decays but reduces ordinary triggers by a sufficiently large factor to avoid writing an unmanageable amount of data to tape. The other is whether the backgrounds can be made small by applying various analysis cuts and making improvements in the spectrometer which reduce the backgrounds seen in existing data. The answer to both questions is "Yes". The total number of triggers expected is $78 \times 10^6$, about twice the number taken in the E555 run in 1982. The backgrounds seen after all cuts and apparatus changes are small and lie well away from the area populated by true $\Xi^\circ \rightarrow p\pi^-$ events on a scatter plot of the mass of the $p$-$\pi^-$ system versus a target pointing variable, $r^2$, to be defined in the text. While it is impossible to say there will be no background when the data sample is multiplied by 1000, indications are that it will not be large in the region of interest.

## Description of the Apparatus, Including the First Level Trigger Selection

The experimental set-up is shown in plan and elevation view in Figure 1(a) and 1(b), respectively. The proton center beam, deflected in the vertical plane by an upstream vernier, is restored to the neutral hyperon beam target by a set of three 3-meter-long dipoles, labeled M1, placed just upstream of the hyperon magnet. This magnet string is the same as that used for E495[10] in the M2 beam line. The maximum production angle is 4 mrad for a beam momentum of 1000 GeV/c. A 1 mm. square 1/2 interaction length beryllium target is used to produce the neutral beam. The 2 mm. diameter collimator used to define the beam in the hyperon magnet, M2, is assumed to be the one that was constructed for the E619 run last spring. The spectrometer which detects the charged particles from the hyperon decays is also essentially the same as that used for E619. Since the decay of interest has a high Q-value and thus a high maximum transverse momentum, the distances between the spectrometer elements, including the two conventional BM109 magnets, M3 and M4, have not been increased as would be expected with the beam energy. Also, the magnetic field in these magnets is proposed to be lower than for E619, operating at a total $p_T$ for the pair of 1.4 GeV/c. This field is sufficient to bend the positive and negative tracks from a $\Xi^\circ \rightarrow p\pi^-$ decay to opposite sides of MWPC5 for any orientation of the decay plane and position of the decay vertex within the decay volume defined by the veto counter, V, and MWPC1. This condition must be met, since correlated x-hits for both decay tracks are needed in the last two downstream MWPC's for the second level trigger processor calculation. These two chambers are offset from the center line toward the pion side in x to maximize acceptance for $\Xi^\circ \rightarrow p\pi^-$ decays where both the pion and the proton strike the chambers. A 40 m. long low pressure helium Cerenkov counter, constructed by adding a 30 m. long by .65 m. diameter snout to the 11 m. Cerenkov counter used in E495, is placed behind the spectrometer centered along the positive track direction. It will operate at a pressure of 103.23 mm. Hg. for a proton threshold of 300 GeV/c and a pion threshold of 45 GeV/c and will be used in veto in the first

level trigger selection. Since all $K_s \to \pi^+\pi^-$ decays accepted by the spectrometer as shown have $\pi^+$ momenta above threshold, they will be rejected with an efficiency of approximately 97% based on our previous experience with this Cerenkov counter. The chamber marked MWPC1 has signal wires with 1 mm. spacing to compensate to some extent the loss in target pointing resolution relative to the 400 GeV/c experiments due to the higher average momentum of the decays. All others have 2 mm. spacing. The counter marked T covers the entire proton hit side of MWPC6. It is used to sharpen the time resolution of the first level trigger, which is expected to be:

$$\text{"GE"} = \overline{V} \cdot \text{MWPC1} \cdot \text{MWPC5 (L} \cdot \text{R)} \cdot \text{MWPC6 (L} \cdot \text{R)} \cdot \text{T} \cdot \overline{C}$$

## The Second Level Trigger Processor

The MWPC signals are received on amplifier cards at the chambers, which "OR" four adjacent wire signals and send out a pulse as the leading edge of a one-shot for use in fast trigger logic. The signals for every card in MWPC5 and MWPC6 will be sent to the counting house and will be latched, as will the data at the chambers for all MWPC's, whenever the first level trigger, "GE", is satisfied. The latched signals from the two rear chambers will be split and used in two ways in the second level trigger decision.

One set of signals will go to linear adders, and window discriminators will be used as in E623[11] to select on hit multiplicity, choosing only events where one and only one hit was received in the left, right, top, and bottom of MWPC's 5 and 6. This requirement removes major sources of unwanted triggers, in particular $\gamma$ pair conversions, which have 2 tracks collinear in y, and vees with missing or extra hits in the two MWPC's used in the calculation to be described below, which often appear to have larger opening angles or momenta because of incorrect hit associations. There is a loss of good data because of these requirements. It was estimated to be a factor of two in the E555 high rate test run to be described later and is accounted for in the request for beam.

The second set of signals will be priority encoded to give the card number of the hit in each chamber section. These will be used to calculate the product of the two momenta and the opening angle squared as approximated by:

$$P_+P_-\theta^2 \approx \frac{k^2\{[(\bar{X}_2+X_2)(Z_1-Z_B)-(\bar{X}_1+X_1)(Z_2-Z_B)]^2+[(\bar{Y}_1+Y_1)-(\bar{Y}_2+Y_2)](Z_B-Z_D)]^2\}}{\{X_2(Z_1-Z_D)-X_1(Z_2-Z_D)\}\{\bar{X}_2(Z_1-Z_D)-\bar{X}_1(Z_2-Z_D)\}}$$

where $k = p_T$ of the magnet and $Z_D$, $Z_B$, $Z_1$, and $Z_2$ are the positions along the beam line of the decay vertex, bend center of the magnets, MWPC5, and MWPC6, respectively.[12] The decay vertex is chosen to be the center of the decay volume, which approximates the vertex for most events more closely than it can

be calculated using the y-hits with the 4 wire (= 8 mm.) segmentation. The x's and y's are the horizontal and vertical coordinates measured outward from the center in the two chambers, i.e., the card numbers. The subscript 1 refers to MWPC5, the subscript 2 refers to MWPC6, and the bar indicates the negatively charged track hits in x; the y-hits do not need to be associated with the x-hits in the calculation, so in this case the bar will refer to, e.g., the hits in the bottom section of each chamber.

The high speed with which the algorithm can be calculated is due in large part to the high degree of parallelism which is possible. The is manifest in Figure 2, which shows the number of calculations going on in each time slot, the type of calculation being performed, and the number of bits used. The calculation time is estimated to be less than 500 nsec. allowing 100 nsec. for multiply and 50 nsec. for add or subtract. An additional dead time of 500 ns for cable delay and priority encoding is assumed in obtaining the estimate of 1 μsec. total dead time for each "GE" accepted by the first level trigger. This includes the cable time needed to clear the data at the chambers in case the second level trigger is not satisfied.

Figure 3 shows the results of the calculation for Monte Carlo events for the two most common decays in the neutral beam, $\Lambda \rightarrow p\pi^-$ and $K_s \rightarrow \pi^+\pi^-$, and for $\Xi^\circ \rightarrow p\pi^-$ decays. Zero on the graph represents $P_+P_-\theta^2 = .2$, and all events with values greater than or equal to this will be accepted. The relative normalization on this histogram does not reflect the actual relative numbers of events of each type accepted by the first level trigger, but shows the number which are accepted by "GE", excluding the $\bar{C}$ cut, for 10,000 events of each type generated in the decay volume. The $\bar{C}$ counter reduces the number of $K_s$'s by a factor of .03 and cuts $\Lambda$'s and $\Xi$'s with proton momenta above 300 GeV/c by the same factor. The overall acceptances for the Monte Carlo events relative to production at the target including both the first and second level trigger are:

| | |
|---|---|
| $\Lambda \to p\pi^-$ | $3.21 \times 10^{-4} \times .642$ |
| $K_s \to \pi^+\pi^-$ | $1.04 \times 10^{-3} \times .6861$ |
| $\Xi^\circ \to p\pi^-$ | $8.91 \times 10^{-2} \times$ B.R.. |

In order to verify that real triggers will be suppressed by as large a factor as the Monte Carlos predict, a study was performed on 1018 raw data triggers from E440,[13] of which only 42.4% are $\Lambda \to p\pi^-$ and 21.9% are $K_s \to \pi^+\pi^-$. Data and Monte Carlo events for $\Lambda \to p\pi^-$ and $K_s \to \pi^+\pi^-$ were subjected to equivalent acceptance windows and to the hit requirements proposed above, and, in the case of the data, to the $\bar{C}_v$ veto. The Cerenkov counter was part of the apparatus used in E440, although it was not used as part of the trigger. The signal appeared as one bit in a gated latch which was read for every trigger and thus was available for use in an offline test. The second level trigger algorithm was calculated for all events which satisfied the "GE" and hit multiplicity requirements. Only three of the 1018 triggers, all of which were $\Lambda \to p\pi^-$, passed all tests including $p_+p_-\theta^2 \geq .2$. The expected numbers from the Monte Carlos, including the measured $\bar{C}_v$ efficiency of 97%, were two $\Lambda$'s and one $K_s$, which is in good agreement.

Very few of the triggers which are not vees pass even the first level trigger. A large fraction is $e^+e^-$ pairs from $\gamma$-ray conversions, which, when they do have an $e^+$ with high enough momentum to hit the narrow allowed positive track x-hit region in MWPC6, will fire the $\bar{C}_v$ counter 97% of the time. The few remaining pairs are killed by the requirement that there be one and only one hit on either side of the horizontal center line in the two downstream MWPC's or by the $p_+p_-\theta^2$ cut. The only other category of non-vee triggers significant enough to mention is events with more than two tracks, which are removed by the $\bar{C}_v$ veto or by the hit requirements in the downstream chambers.

## The E440 $\Xi^0 \to p\pi^-$ Analysis

To test the feasibility of a rare mode search in the neutral hyperon apparatus, a $\Xi^0 \to p\pi^-$ analysis was performed on the E440 data using the compacted 7.2 mrad production angle data tapes. These contain all events which reconstruct as neutral vees, approximately 68% of the raw triggers for this sample. A similar set of cuts to those applied in selecting $\Lambda$'s for the polarization and magnetic moment analysis of these data were imposed. Only events with a sufficient number of chamber hits on them to assure a good vee fit and with large enough opening angle to assure unambiguous association of x and y views were used in the analysis. About 92% of the vees on the compacted tapes satisfied these criteria. Then, only vees for which the positive track momentum was greater than the negative track momentum were selected, since this is true for all $\Xi^0 \to p\pi^-$ decays and for all $\Lambda \to p\pi^-$ decays used in normalization. To eliminate most of the events produced by interactions in the decay pipe windows, the decay vertex was required to be inside the decay volume and at least one standard deviation away from either window using the measured error in the vertex position for that event. Vees produced on a known source upstream of the hyperon beam target were eliminated by making a cut on the angle of the vee momentum vector relative to the beam centroid in the vertical plane at $\pm$ 1.25 mrad. Also, the momentum of the vee was required to be greater than or equal to 50 GeV/c, since below that the efficiency corrections are large and hard to estimate. The invariant mass and error in mass were calculated for all vees which met the above criteria assuming both $p$-$\pi^-$ and $\pi^+$-$\pi^-$ particle identification.

Events with masses within three standard deviations of the $\Lambda$ mass using the mass error as calculated for each event were used for normalization. To eliminate non-target-produced $\Lambda$'s, including daughter $\Lambda$'s from $\Xi^0 \to \Lambda\pi^0$ decays, from the sample, the $\Lambda$ momentum vector was extrapolated back along the beam direction to the hyperon target where it was required to intersect a plane perpendicular to

the beam direction within a circle of radius squared, $r^2$, equal to .4 $cm^2$. The total of $3.083 \times 10^6$ $\Lambda$'s thus collected must be corrected downward for an estimated background of .5% $K_s$'s and .1% $\Xi^\circ$ daughters to $3.065 \times 10^6$.

To search for possible $\Xi^\circ \rightarrow p\pi^-$ events, the track momenta, vertex position, target pointing information, and masses with errors were printed out for all vees remaining after the initial set of cuts which had $p\text{-}\pi^-$ mass greater than or equal to 1.25 GeV and $\pi^+\text{-}\pi^-$ mass greater than or equal to .56 GeV. About ten such events were printed out for each of the 69 raw data tapes included in the sample. This number was reduced to about three per tape by making a cut in the target pointing variable well outside the cut made on the $\Lambda$'s at $r^2 = 1.5$ $cm^2$, and the events with values of $r^2$ smaller than this were studied for clues as to their origin.

One category of background stood out quite clearly in these data. These were events where the positive track had a much higher momentum than the negative. The total number of such events and their $p\text{-}\pi^-$ mass distribution in the region being investigated agreed with Monte Carlo calculations for $\Lambda \rightarrow pev$ decays when they were misidentified and reconstructed as vees with this mass hypothesis. A cut was made on P+/P-, and events with values of this ratio less than 18 were retained for further study. According to Monte Carlo calculations, this removes all of the $\Lambda \rightarrow pev$ decays which fall in the high $p\text{-}\pi^-$ mass region but only .3% of the $\Xi^\circ \rightarrow p\pi^-$ decays otherwise accepted.

Figures 4, 5, and 6 are scatter plots of $m_{p\pi}$ and $m_{\pi\pi}$ versus the target pointing variable and $m_{p\pi}$ versus $m_{\pi\pi}$ for the total of 146 events from the entire data set which survived all the cuts enumerated above. Events with $.56 \leq m_{\pi\pi} < .58$ are circled on the figure where this variable is not manifest. It is clear from the concentration of points at the lowest $\pi^+\text{-}\pi^-$ masses and toward larger values of $r^2$ in Figure 5 that most of the background comes from $K_s \rightarrow \pi^+\pi^-$ events in which one of the tracks scatters or decays or in which

there are missing or extra hits and thus mistakes in reconstruction. These effects cause them to be shifted to higher masses and to not point back to the target.

The projected mass and target pointing distributions for the data are shown on Figure 4 along with the same distributions for the Monte Carlo $\Xi^\circ \to p\pi^-$ events. 98.6% of true $\Xi^\circ \to p\pi^-$ events which satisfy all other requirements fall in the region marked I on the plot. Three background regions with the same area are selected, marked II, III, and IV, all of which are within the kinematic limit for the $K_s \to \pi^+\pi^-$ events on the $m_{p\pi}$-axis as is evident on Figure 6, so that the expected background is constant over the four regions. The target pointing variable is cut at $r^2 = .4\ cm^2$ for all regions as for the beam $\Lambda$'s.

The data were analyzed for two choices of the $\pi^+\pi^-$ mass cut. When this variable is cut at $m_{\pi^+\pi^-} \geq .56$, there are a total of nine events in the four regions including one in region I. The 90% confidence level upper limit on the expectation value $\bar{N}$ for true $\Xi^\circ \to p\pi^-$ events is obtained using Poisson statistics by solving:

$$.1 = \frac{\int_0^\infty P(b,9)\ \dfrac{\sum_{i=0}^{1} P(b/4,1-i)\ P(\bar{N},i)}{\sum_{i=0}^{1} P(b/4,1-i)}\ db}{\int_0^\infty P(b,9)\ db} \qquad \text{(Ref. 1)}$$

This yields $\bar{N} = 2.7$, and the corresponding upper limit on the branching ratio for such events is calculated from the relation:

$$\frac{\Gamma(\Xi^\circ -)p\pi^\circ}{\Gamma(\Xi^\circ \to \Lambda\pi^\circ} = \frac{\left(\frac{2.7}{.04280}\right)}{\left(\frac{3.065\times10^6}{.1498\times.642}\right)\left(3.6\times10^{-2}\right)} = 5.5\times10^{-5}$$

where .04280 is the overall efficiency for detection of $\Xi^\circ \to p\pi^-$ events after all cuts, .1498 is the detection efficiency for the beam $\Lambda$'s as they were selected, .642 is in the branching ratio for $\Lambda \to p\pi^-$ and $3.6 \times 10^{-2}$ is the relative number of $\Xi$'s to $\Lambda$'s produced at the target at this production angle. The latter number was obtained from E495 data using fully reconstructed $\Xi^\circ \to \Lambda\pi^\circ$ decays and was confirmed by studying the $\Lambda \to p\pi^-$ events in the E440 data which do not point back to the hyperon target, i.e., events for which the target pointing variable, $r^2$, defined above is large.

When the $m_{\pi^+\pi^-}$ cut is made instead at .58, there are five events in the four regions and none at all in Region I. The 90% c.l. upper limit on $\overline{N}$ becomes 2.3 and the efficiency for Detection of $\Xi^\circ \to p\pi^-$ is reduced to .03933 by the more restrictive cut on the allowed $\pi^+\pi^-$ mass region. Then, the branching ratio calculation yields:

$$\frac{\Gamma(\Xi^\circ \to p\pi^\circ}{\Gamma(\Xi^\circ \to \Lambda\pi^\circ} = \frac{\left(\frac{2.3}{.03933}\right)}{\left(\frac{3.065\times10^6}{.1498\times.642}\right)(3.6\times10^{-2})} = 5.1\times10^{-5}$$

which is a somewhat smaller upper limit.

The discussion of the E440 data would not be complete without addressing the subject of background reduction. The major source of background is $K_s \to \pi^+\pi^-$ decays which reconstruct with a mass many standard deviations from the true $K_s$ mass. A sample of 100,000 Monte Carlo $K_s \to \pi^+\pi^-$ decays were generated and subjected to the same analysis requirements as the beam $\Lambda$'s, and none of these events reconstructed with masses above .56 GeV. The Monte Carlo program did allow for $\pi \to \mu\nu$ decays and for multiple Coulomb scattering of the pions in a 1/8" scintillation counter placed behind the most upstream MWPC for purposes of making the trigger more precise in time, but neither of these effects was sufficiently large to shift the $K_s$'s to such apparently high masses. A subset of vees from the high mass region with no missing or extra hits in any of the first 5 MWPC's for which reconstruction

mistakes were not the likely cause of the mass shift were studied to see if a scatter in the timing counter on one of the tracks, which to first order would change the opening angle of the vee but not the track momentum, could be one source of high mass events. It was found that the magnitude of the shift in target pointing, $\Delta r$, could be reliably predicted from the shift in mass, $\Delta m$, assuming that the event was a $K_S \rightarrow \pi^+\pi^-$ decay and that the track with the scatter was the one that shifted the target pointing variable in the measured direction. The timing counter is placed behind MWPC6 in the proposed experiment where it will not affect the charged track measurements.

The $\bar{C}^v$ information has not been used in the analysis because the negative tracks for some of the true $\Xi^\circ \rightarrow p\pi^-$ decays and for some of the beam $\Lambda \rightarrow p\pi^-$ decays as well could have fired the counter, which was large and centered on the neutral beam line. A detailed study of efficiency versus position, angle, and energy for pions would have to be performed to determine the reduced efficiency for the decays of interest. The small number of background events made this unnecessary for the purposes of the E440 analysis.

The information is useful, however, in studying expected backgrounds in the proposed experiment. The $\bar{C}^v$ counter in this case will be smaller in diameter over 3/4 of its length and will see only the positive particles from the decays. The decay vertex distributions for background events with and without a $\bar{C}^v$ signal are shown in Figure 7 (a) and (b) for comparison. The shaded region under each curve denotes the events included in the sample for which the target pointing variable, $r_j^2$ was less than .4 $cm^2$. It is clear that a large fraction of the events which remain after a $\bar{C}^v$ cut are produced in the window of the decay pipe. The veto counter will be placed inside the decay pipe and thus behind the window to reduce this background source. Figure 8 shows the $p\text{-}\pi^-$ mass versus the target pointing variable for the events shown in Figure 7(b) with Z vertex $\geq$ 3m. to demonstrate the character of the expected background for the proposed experiment. The events with $.56 \leq m_{\pi\pi} < .58$ are circled to show which events

would be removed by a more stringent $K_s$ cut. The regions populated by background lie well away from the areas of interest for true $\Xi^\circ \rightarrow p\pi^-$ decays, which indicates that the backgrounds will be manageable for the more sensitive test.

Request for Beam Time

A high rate test tape was taken during the E555 running period at a production angle of 7.5 mrad and an incident beam energy of 400 GeV/c. This is equivalent in $P_T$ to 3 mrad at 1000 GeV/c, the assumed production angle and beam energy for the proposed experiment. The spectrometer was set up for E555 in the M2 beam line in the Meson Lab in essentially the same configuration as it was for E440. The "GE" trigger for the test run required a hit in MWPC1, one on either side of MWPC5 in X, a signal in the timing counter on the back of MWPC1, and no signal in the veto that defines the start of the decay volume. An instantaneous beam intensity of $1.2 \times 10^{10}$ protons/sec. on the 1/2 interaction length beryllium target resulted in an ungated rate of 50,000 "GE's" per second in the spectrometer. Since all of these are at least two track events, no less than 100,000 charged particles per second traverse the upstream chambers. In the proposed experiment these will strike only a few wires in each plane because of the small size of the collimator (2 mm) to be used to define the neutral beam and the low Q-value of the most common triggers. Thus the rates on these wires will be close to the space charge limit of $3 \times 10^4$ charged particles/cm/sec/wire[14] at the equivalent of the test run beam intensity correcting for the different primary energy and the different collimator size and location. The Proton Center hyperon magnet is longer than its Meson Lab counterpart and the defining collimator is 1.5 times further from the target and it is smaller in diameter by a factor of two. The beam intensity must be higher by a factor of 9.2 to correct for the solid angle difference. The inclusive production spectrum as a function of x and $p_T$ is:

$$\frac{d\sigma}{dx d\Omega} = x\left(p_{max}\right)^2 f(x,p_T).$$

Thus, when the primary energy is raised from 400 GeV to 1000 GeV, there is an increase in the secondary beam through the collimator at fixed x for bin width $\Delta x$ of $(2.5)^2$. The running intensity must therefore be corrected downward

by a factor of 6.25. The requested intensity for the proposed experiment is $1.76 \times 10^{10}$ protons/sec after these corrections are applied. This integrates to $3.5 \times 10^{11}$ protons over the expected 20 second spill.

The production spectra for $\Lambda$'s, $K_s$'s and $\Xi^0$'s as a function of x at the equivalent angle and the number of each produced relative to protons on target integrating from 50 to 400 GeV/c were determined from the E440 and E495 data. This information was used in generating $\Lambda \rightarrow p\pi^-$ and $K_s \rightarrow \pi^+\pi^-$ Monte Carlos for the proposed experimental set-up to test the effect of the first level trigger on these decays and thus their contribution to the rate the second level trigger processor must handle. The overall rate to the processor must include the other raw triggers which pass the first level selection criteria. The total was estimated to be about 18,300/sec. adding in the expected additional triggers using the information obtained in the E440 raw trigger study. The percent contribution of the vee triggers to the total is 75% $\Lambda$'s and 3% $K_s$'s. None of the non-vee triggers satisfied both parts of the second level trigger according to the study. Thus the $\Lambda$ and $K_s$ Monte Carlos are assumed to predict correctly the number of events that will be collected and written to tape after both levels of trigger selection are applied. This number is estimated to be 217/sec., of which 76% are $K_s$'s and 24% $\Lambda$'s. In addition, a number of prescaled "GE" triggers omitting the $\bar{C}_v$ veto requirement will be written to tape for normalization purposes. Without the $\bar{C}_v$ veto there are 40,400 triggers/sec. These will be prescaled by 2048 and will thus add 20 events/sec. to the number written. The $\bar{C}_v$ signal will be included in a gated latch for every such event to provide a monitor of its efficiency. The second level trigger signals will also be latched for these prescaled events to provide a means of checking the efficiency of these elements of the trigger off-line.

Since the expected number of events written to tape per second is only 237, which is well below the throughput of the 1600 bpi tape drive on the on-line computer, no write dead time is incurred. The dead time per second estimate can be obtained as the sum of the second level trigger dead time of 1 μsec. multiplied by 18,300 "GE's" per second which equals .018 sec/sec. and the CAMAC event read dead time of 300 μsec. multiplied by the 237 events read per second which equals .071 sec/sec. Thus the experiment will be live 91% of the time.

The total number of $\Lambda$'s produced at the target per second into the collimator solid angle at the requested running intensity correcting for dead time is $233 \times 10^3$. Multiplying by the $\Xi^\circ/\Lambda$ ratio of .036, there are $8.4 \times 10^3$ $\Xi^\circ$'s produced per second. The efficiency for detecting a true $\Xi^\circ$ produced at the target for a branching ratio of 100% is .036. This includes the lifetime, the geometric efficiency and $\bar{C}_v$ veto of the first level trigger, the second level hit requirements, $p_+p_-\theta^2 \geq 2$ from the processor algorithm, and all the analysis cuts enumerated for the E440 analysis including the mass and target pointing cuts as estimated from Monte Carlo $\Xi^\circ \rightarrow p\pi^-$ decays. An additional data reduction factor of 1/2 was obtained by comparing the E440 reconstructed $\Lambda$ and K yields to the E555 high rate tape yields, and imposing the hit requirements of the second level trigger. Thus the number of $\Xi^\circ \rightarrow p\pi^-$ events detected in a 20 sec. spill for a branching ratio of 100% is $8.4 \times 10^3 \times .036 \times 20 = 6048$ /spill. For a branching ratio of $10^{-8}$ the number is $6048 \times 10^{-8}$/spill. Taking the reciprocal, the number of spills needed to collect one event if the branching ratio is $10^{-8}$ is 16534. At 60 spills per hour this corresponds to 276 hours of running time. The request for 500 hours includes time for beam tuning and time for timing in and testing the apparatus including the trigger processor.

Computer Time Request

The total number of triggers collected is expected to be $78 \times 10^6$. The CPU time estimate for processing the raw data tapes can be obtained from the E555 analysis since the data structure is almost identical for the two experiments. There are 150 data tapes for E555 each of which contains about 275,000 triggers. At the first level of processing, the events which reconstruct as vees are written to a compacted tape as in the E440 analysis. This takes 3000 sec. of CPU time per tape. The second level analysis time is expected to be about 1000 sec. of CPU time per tape for the $\Xi^\circ \to p\pi^-$ search. There will be twice as many triggers and thus twice as many tapes for the proposed experiment as for E555. The total CPU time estimate is obtained from 300 tapes times 4000 sec. per tape or 330 hours.

References


1. S.F. Biagi et al., Phys. Lett. 112B, 277 (1982).
2. G. Geweniger et al., Phys. Lett. 57B, 193 (1975).
3. L. Wolfenstein, Phys. Rev. Lett. 13, 562 (1964).
4. M. Konuma et al., Prog. of Theor. Phys. 46, 527 (1971).
5. L.B. Okun', Sov. Journal of Nucl. Phys. $\perp$, 806 (1965).
6. S.L. Glashow, Phys. Rev. Lett. 6, 196 (1961).
7. M. Kobayashi and T. Maskawa, Prog. of Theor. Phys. 49, 652 (1973).
8. S.L. Glashow et al., Phys. Rev. D2, 1285 (1970).
9. Lincoln Wolfenstein, private communication.
10. P.T. Cox, "The Magnetic Moment of the Cascade-Zero Hyperon", PhD. Thesis, University of Michigan, UM HE 80-19 (unpublished).
11. H.C. Fenker et al., "The E623 $\phi\phi$ Trigger Processor", Fermilab preprint, FERMILAB-Pub-82/62-EXP.
12. This is the algorithm used to select high-mass $\mu$ pairs in E400 at Fermilab. See T.F. Droege et al., IEEE Transactions on Nuclear Science, Vol. NS-25, No. 1, Feb. 1978.
13. For complete details on this experiment, see L. Schachinger, "The Magnetic Moment of the Lambda Hyperon", PhD. thesis, Rutgers University, RU-78-108 (unpublished).
14. F. Sauli, "Principles of Operation of Multiwire Proportional and Drift Chambers," CERN 77-09.

## Figure Captions

Figure 1 (a) and (b): Plan and elevation view of the apparatus for the proposed experiment. The production angle is in the vertical plane. Differences between this and the E440 apparatus are the placement of the veto counter, V, which was upstream of the decay pipe window, the placement of the timing counter, T, which was on the rear face of MWPC1, the location of the $\bar{C}_V$ counter, which was between MWPC5 and MWPC6, and the placement of MWPC5 and MWPC6 in X, which were symmetric about the beam center line. The E555 apparatus was set up in the same configuration as E440 but without the $\bar{C}_V$ counter.

Figure 2: Schematic of the second level trigger processor. The algorithm is calculated in parallel wherever possible. The number of calculations and the type of operation performed in each time slot is shown as well as the chip size required for the maximum number of bits and the time estimate per step.

Figure 3: Results of the algorithm calculation for $\Lambda \to p\pi^-$, $K_s \to \pi^+\pi^-$, and $\Xi^\circ \to p\pi^-$ decays. The variable MDIF is defined as:

$$\text{MDIF}/100 = k^2 \{[(\bar{x}_2+x_2)(z_1-z_B)-(\bar{x}_1+x_1)(z_2-z_B)]^2 + [((\bar{y}_1+y_1)-(\bar{y}_2+y_2))(z_B-z_D)]^2\} - (p_+p_-\theta^2)_{min}\{x_2(z_1-z_D)-x_1(z_2-z_D)\}\{\bar{x}_2(z_1-z_D)-\bar{x}_1(z_2-z_D)\},$$

with $k^2 = 1.96$ and $(p_+p_-\theta^2)_{min} = .2$. See the text for a definition of all the quantities used in the calculation. All events with MDIF $\geq 0$ will be accepted by the processor.

Figure 4: Invariant mass assuming the $p\text{-}\pi^-$ mass hypothesis versus the target pointing variable, $r^2$, for the 146 events which pass the E440 analysis cuts including well-fit unambiguous vee, stiff positive track, vertex at least one standard deviation from decay pipe windows, vee momentum $\geq$ 50 GeV/C, positive track momentum divided by negative track momentum less than 18, vee momentum within 1.25 mrad of beam centroid in y and $m_{p\pi^-} \geq 1.25$ GeV, $m_{\pi^+\pi^-} \geq .56$, and $r^2 < 1.5$ cm$^2$.

Figure 5: Invariant mass assuming the $\pi^+\pi^-$ mass hypothesis versus the target pointing variable, $r^2$, for the same 146 events as in Figure 4. (Three events which have $\pi^+\text{-}\pi^-$ masses well above the kinematic limit for true $\Lambda^0 \to p\pi^-$ events are omitted when this variable is plotted.)

Figure 6: Invariant mass for the $p\text{-}\pi^-$ mass hypothesis versus invariant mass for the $\pi^+\text{-}\pi^-$ mass hypothesis for the same 146 events as in Figure 4.

Figure 7: Decay vertex distribution for the 146 events plotted in Figure 4. The events for which the $\check{C}^v$ fired are shown in (a) and those for which it did not in (b). The shaded region under each plot shows the number of these events for which $r^2 < .4$.

Figure 8: Invariant mass assuming the $p\text{-}\pi^-$ mass hypothesis versus the target pointing variable, $r^2$, for the 17 background events which appear in Figure 7(b) for which $Z \geq 3m$.

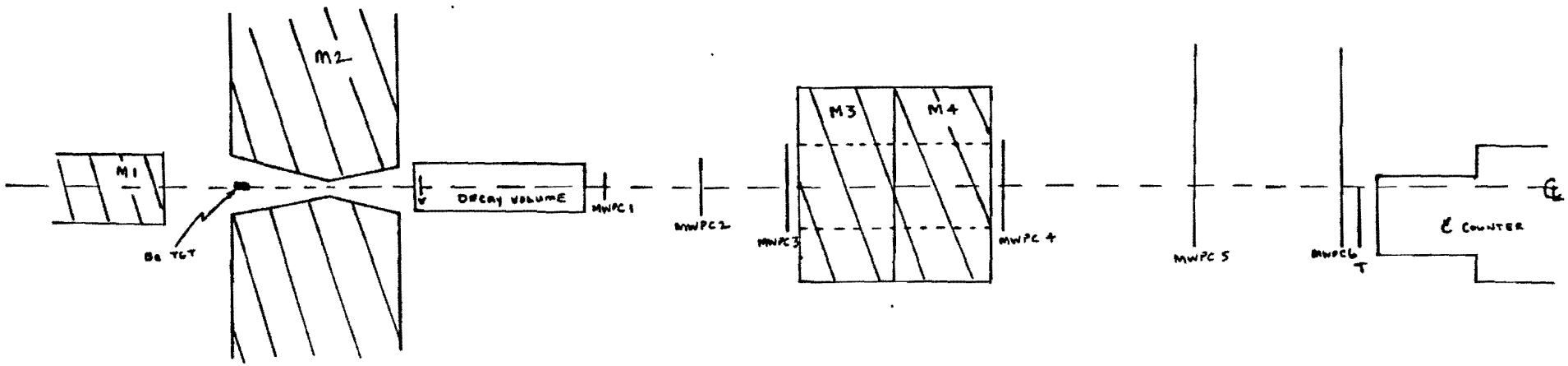
M1
M2
M3
M4
Be TGT
Decay volume
MWPC 1
MWPC 2
MWPC 3
MWPC 4
MWPC 5
MWPC 6
T
ℓ COUNTER

(a)

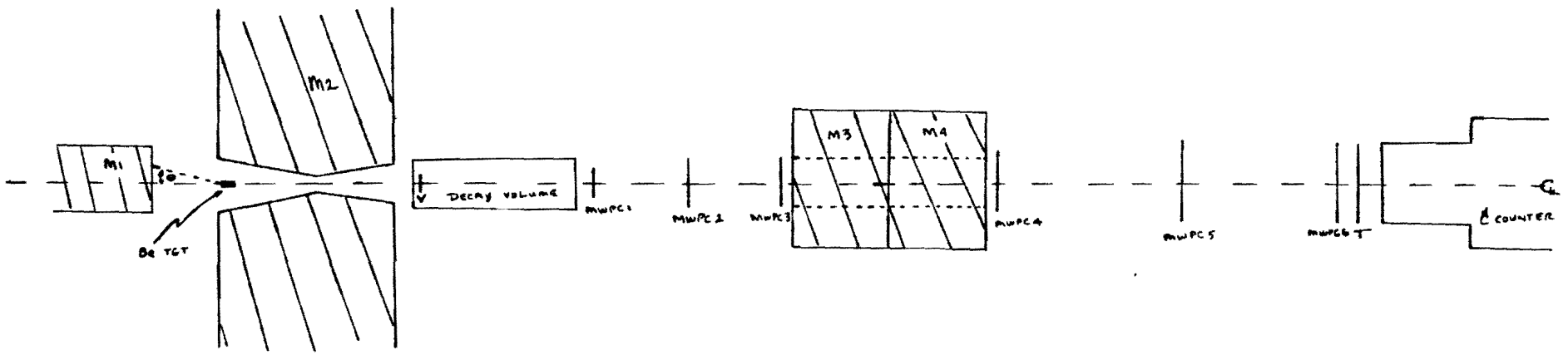
M1
M2
M3
M4
Be TGT
Decay volume
MWPC 1
MWPC 2
MWPC 3
MWPC 4
MWPC 5
MWPC 6
T
ℓ COUNTER

(b)

FIGURE 1

| TIME SLOT | OPERATION | # OF SIMULTANEOUS CALCULATIONS | CHIP SIZE | ESTIMATED TIME (nsec) |
|---|---|---|---|---|
| 1 | ADD | 4 | 8 + 8 | 50 |
| 2 | MULTIPLY | 8 | 8 x 8 | 100 |
| 3 | SUBTRACT | 4 | 16 + 16 | 50 |
| 4 | MULTIPLY | 3 | 12 x 12 | 100 |
| 5 | ADD | 2 | 16 + 16 | 50 |
| 6 | MULTIPLY | 2 | 12 x 12 | 100 |
| 7 | COMPARE | 1 | 16 + 16 | 50 |

$\Sigma t = 500$ nsec

FIGURE 2

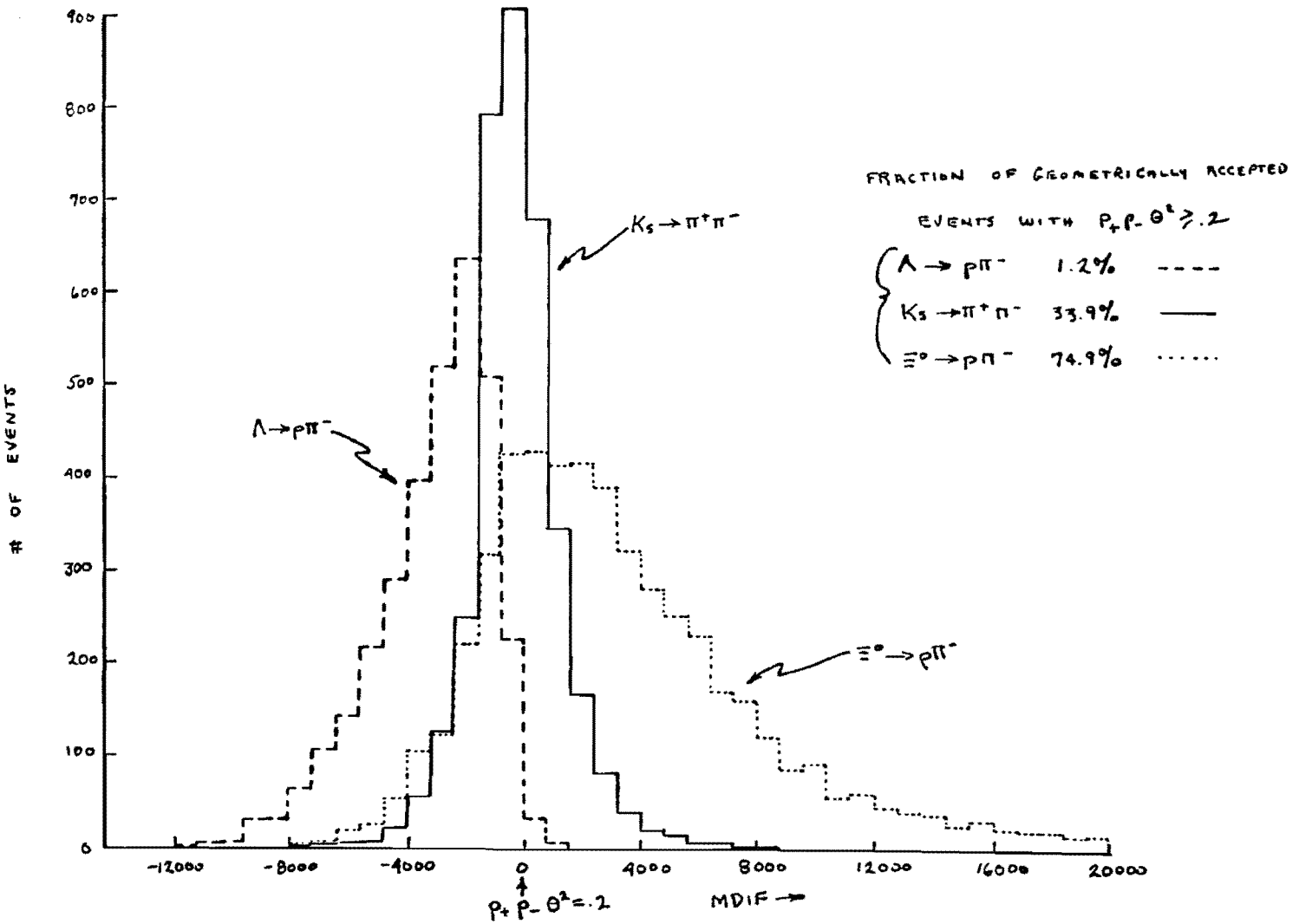
900
800
700
600
500
400
300
200
100
0
# OF EVENTS
$K_S \to \pi^+\pi^-$
$\Lambda \to p\pi^-$
$\Xi^\circ \to p\pi^-$
FRACTION OF GEOMETRICALLY ACCEPTED EVENTS WITH $P_+P_-\theta^2 \geq .2$
$\Lambda \to p\pi^-$ 1.2%
$K_S \to \pi^+\pi^-$ 33.9%
$\Xi^\circ \to p\pi^-$ 74.9%
-12000
-8000
-4000
0
4000
8000
12000
16000
20000
$P_+P_-\theta^2 = .2$
MDIF

FIGURE 3

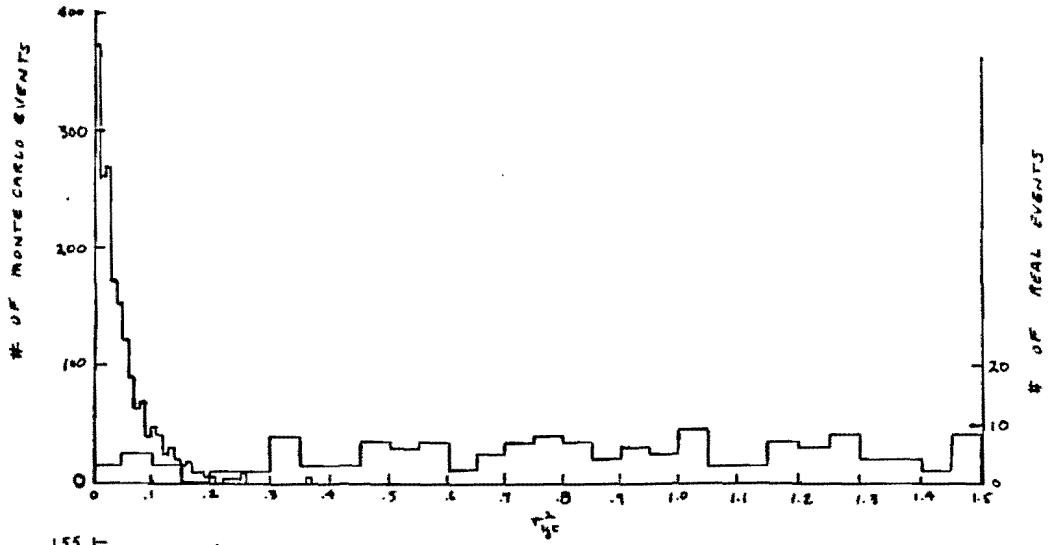
# OF MONTE CARLO EVENTS
# OF REAL EVENTS

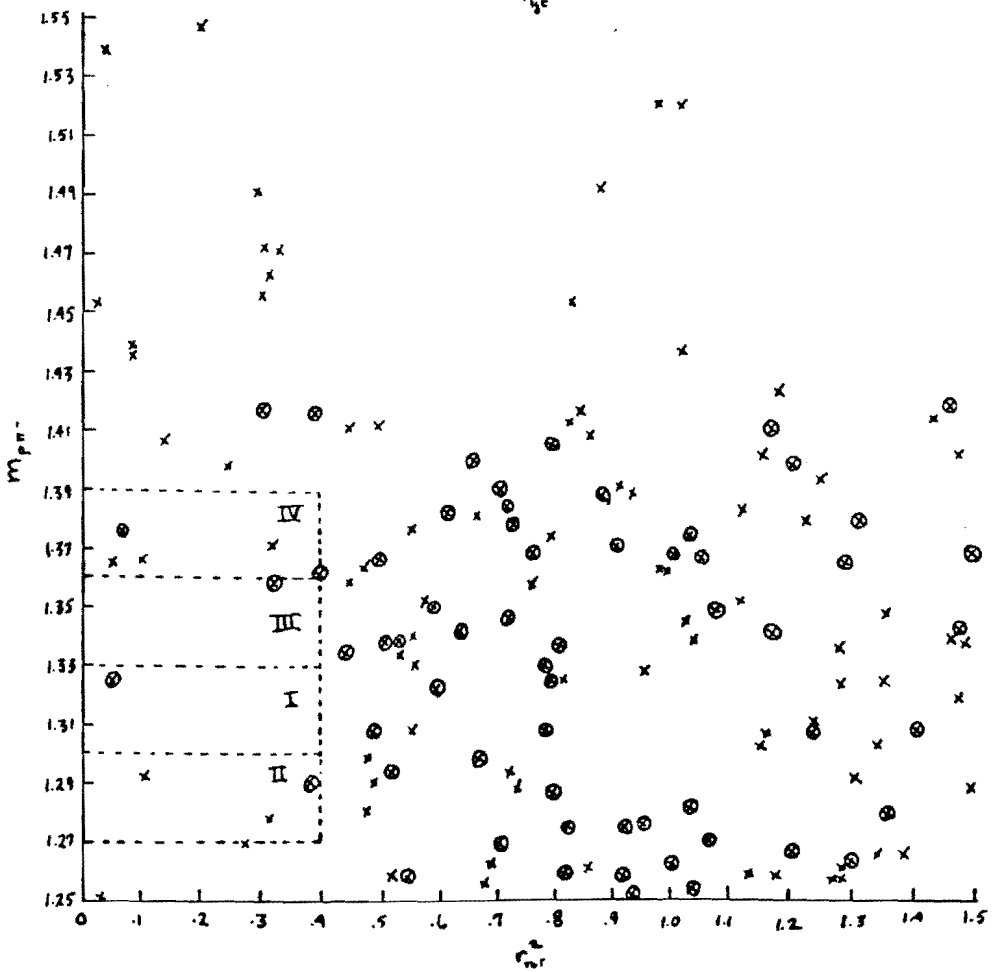
IV
III
I
II

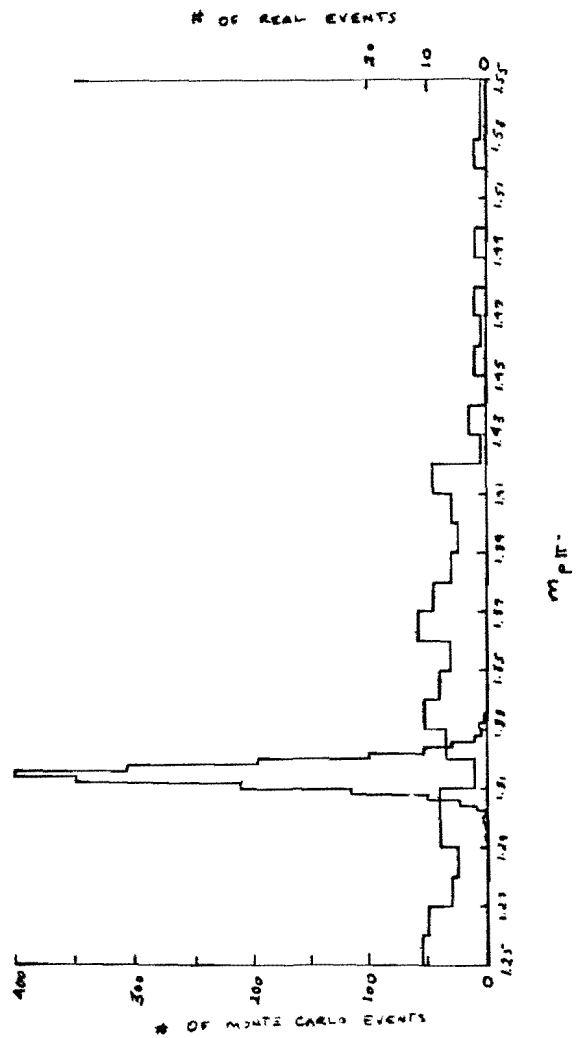
# OF REAL EVENTS
# OF MONTE CARLO EVENTS

FIGURE 4

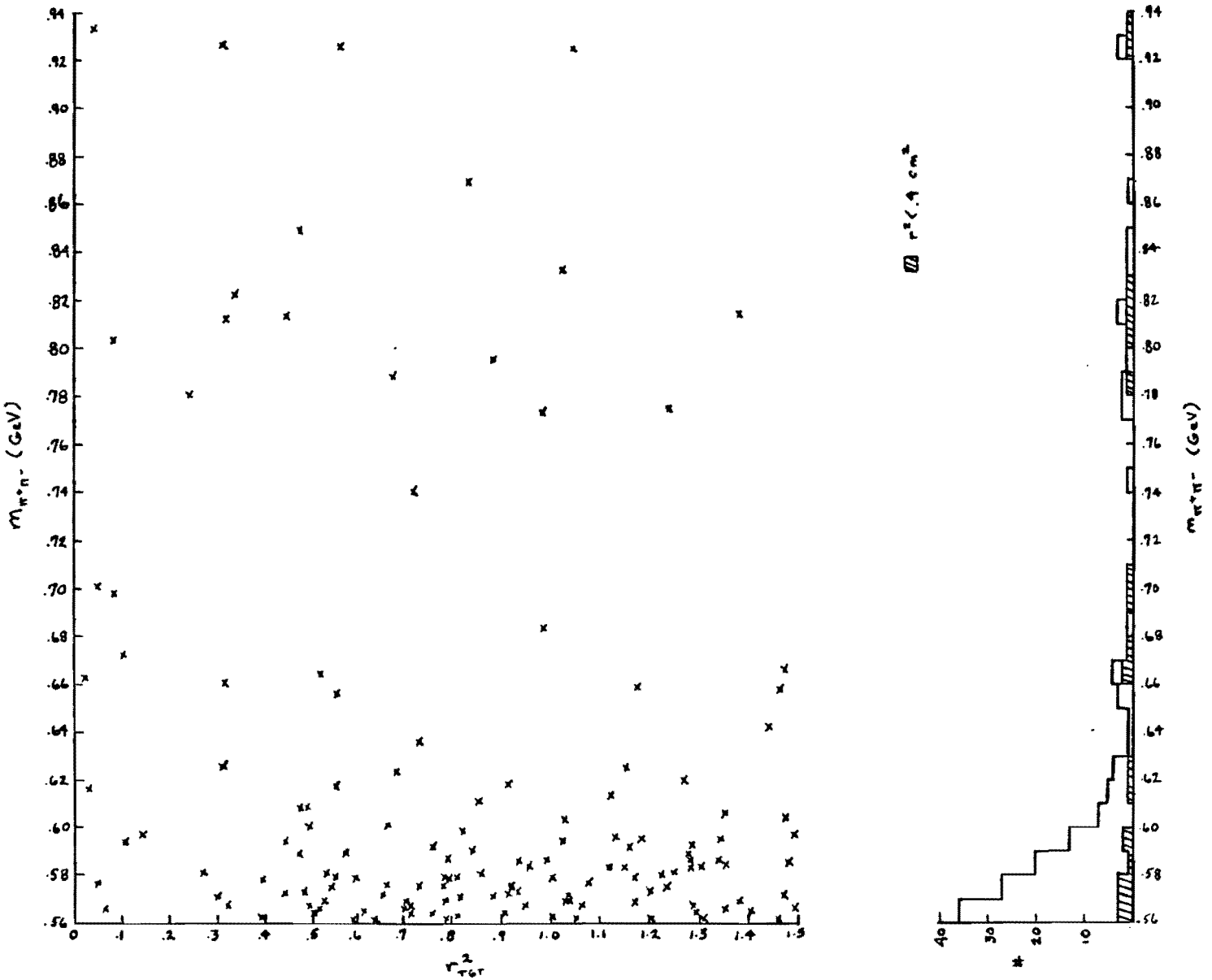


FIGURE 5

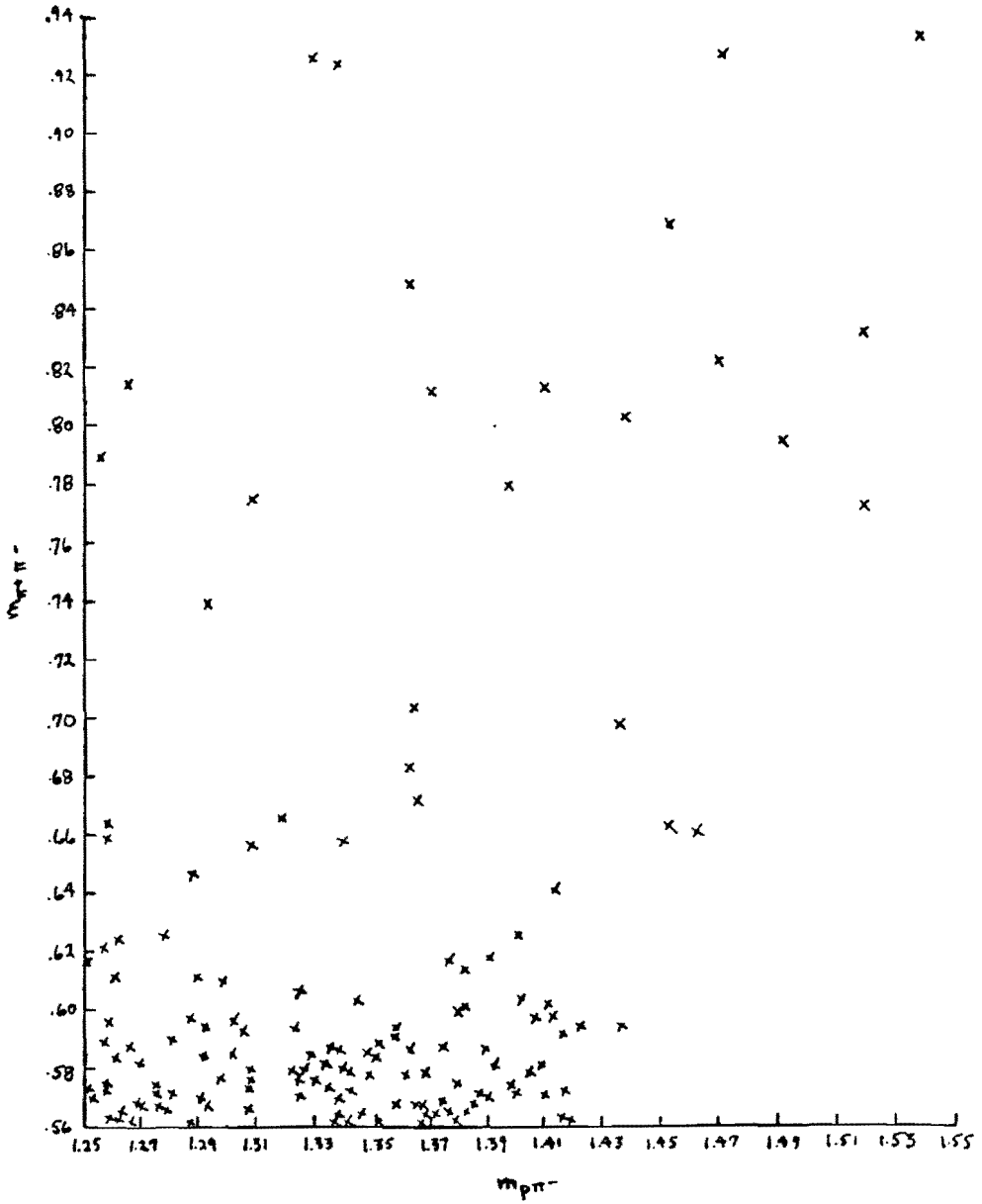
.94
.92
.90
.88
.86
.84
.82
.80
.78
.76
.74
.72
.70
.68
.66
.64
.62
.60
.58
.56
1.25
1.27
1.29
1.31
1.33
1.35
1.37
1.39
1.41
1.43
1.45
1.47
1.49
1.51
1.53
1.55
$m_{p\pi^-}$

FIGURE 6

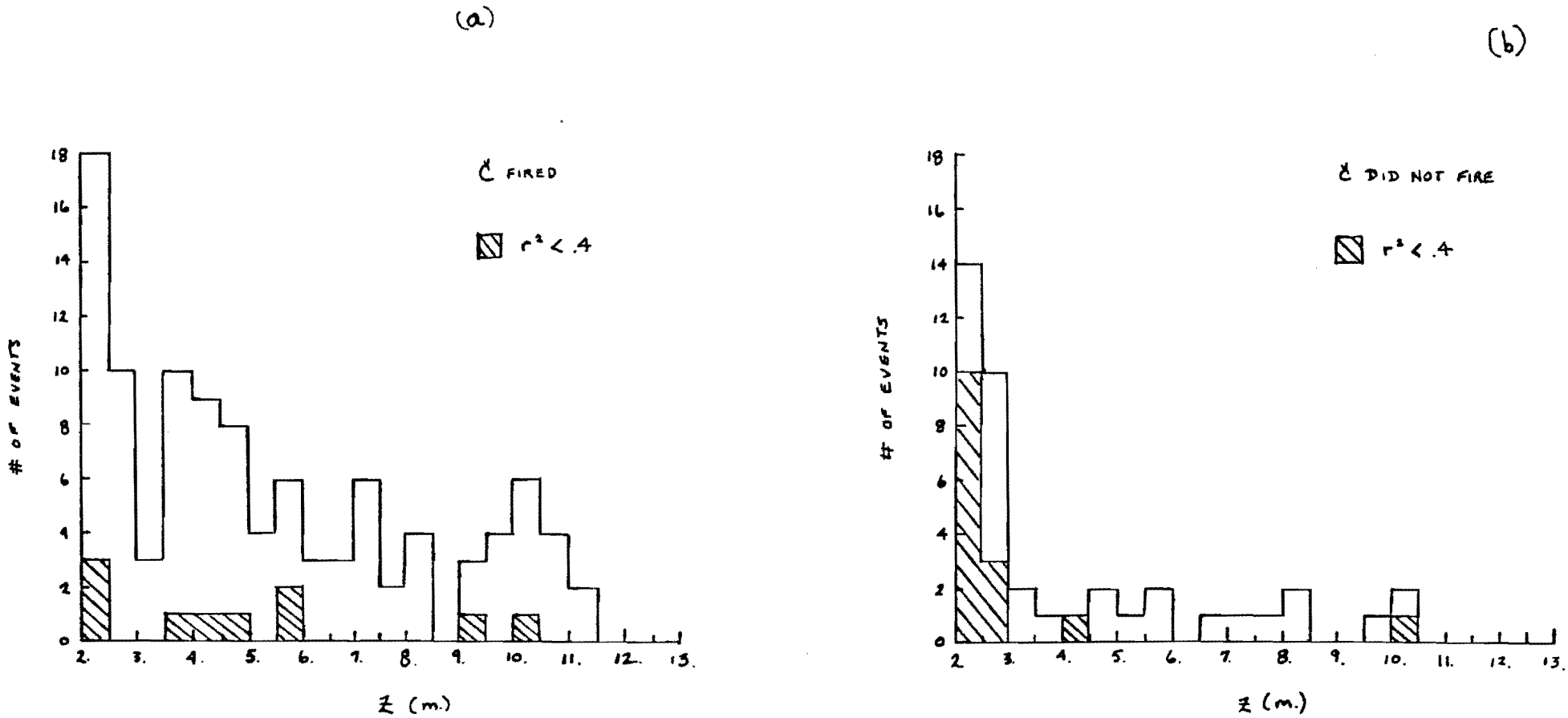
(a)
(b)
Č FIRED
Č DID NOT FIRE
$r^2 < .4$
# OF EVENTS
Z (m.)
0
2
4
6
8
10
12
14
16
18
2.
3.
4.
5.
6.
7.
8.
9.
10.
11.
12.
13.

FIGURE 7

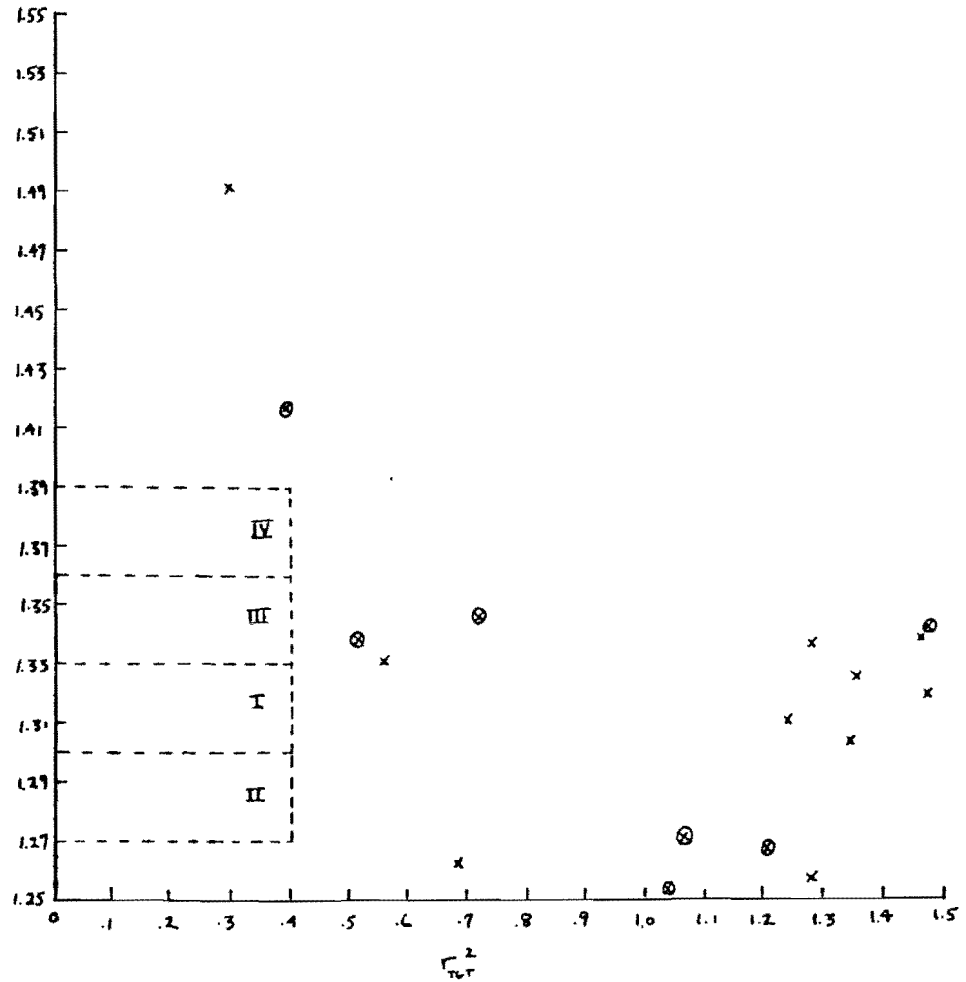
1.55
1.53
1.51
1.49
1.47
1.45
1.43
1.41
1.39
1.37
1.35
1.33
1.31
1.29
1.27
1.25
IV
III
I
II
0
.1
.2
.3
.4
.5
.6
.7
.8
.9
1.0
1.1
1.2
1.3
1.4
1.5
$r^2_{TOT}$

FIGURE 8